# Seismological Re-evaluation of Regional Stress Orientation and Fracture Angle in the Kinki District, South west Japan with Reference to Developmental Process of Conjugate Faults

AUTHOR(S):

NISHIDA, Ryohei; HIRANO, Masashige; SHIONO, Kiyoji

# Seismological Re-evaluation of Regional Stress Orientation and Fracture Angle in the Kinki District, Southwest Japan with Reference to Developmental Process of Conjugate Faults

By Ryohei NISHIDA, Masashige HIRANO and Kiyoji SHIONO

(Manuscript received March 27, 1974)

**Abstract**

The results of studies on focal mechanism of earthquakes in the Kinki district, Southwest Japan are reviewed and re-examined in order to evaluate regional stress orientation, $\Phi$, fracture angle, $\theta_0$, and internal friction, $\mu$, in the crust. Two peaks in the frequency distribution of the azimuth of the P-axis leads us to a conclusion that $\Phi$=N85°E, $2\theta_0$=70°–75° and $\mu$=0.3–0.4. Ratio of inconsistent data given by Hashizume (1970) with the assumed axis of tectonic compression, N85°E, also suggests that $2\theta_0$=70°–80°, in spite of his negative conclusion. These values of $2\theta_0$ are in good agreement with those obtained from joint study of the Rokko Mountains.

Based on the seeming nature of this situation, it is also concluded that defraction of the P-axes near the major faults suggests that fracturing occurs along the plane parallel to the active fault itself and sense of dislocation is concordant with that of the fault. Further, periodic change of the P-axes of the Matsushiro earthquake swarm leads us to a significant aspect on the developmental process of a conjugate fault system.

## 1. Introduction

It has been suggested by Huzita (1969)[1] that there is a close relationship between the linear arrangement of the epicenters of microearthquakes and the trace of the active faults in the northwestern part of the Kinki district. Interrelation of tectonics and seismicity is one of the essential problems concerning the mechanics and process of faulting in the crust.

From this point of view, it is notable that there seem to be two dominant orientations among the strikes of the axes of maximum compression which Ichikawa (1965)[2] gave for the very shallow earthquakes in the Inner Zone of Southwest Japan. Similar characteristic separation of the axial orientation can be observed on the earthquakes belonging to the sequence of the Matsushiro earthquake swarm (Ichikawa, 1969)[3].

If we apply the fault model of earthquake to the interpretation of focal mechanism, we can explain such a fluctuation of the axes of compression, taking into account of the relation between the fault plane and the axes of compression derived seismologically.

Faults in a conjugate set are known geologically to cross each other with an angle less than 90°. When dislocation occurs along one of the possible conjugate fractures, orientation of the axis of maximum compression inferred from the radiation pattern of the initial motions of *P*-waves (the axis is called the *P*-axis in the following) drifts by a half of 90° minus $2\theta_0$ ($\theta_0$; the angle of fracture) from that of the axis of the

actual tectonic stress which is obtained as a bisecting line of the conjugate faults. Because, one of the nodal lines is identical with the plane of faulting. If dislocations occur alternatively along each of the conjugate fractures crossing with an angle smaller than 90°, and if the elastic shocks are observed as earthquakes, the *P*-axis of these earthquakes will have two dominant orientation of $45°-\theta_0$ and $-45°+\theta_0$.

Generally speaking, whenever the angle between the fault plane and the axis of maximum compression of the actual tectonic stress is not equal to 45°, the *P*-axis differs from the axis of the real maximum compression. On the contrary, careful examination of these drifts may provide us a key to interpret the characteristics of fractures in the Earth's crust.

A similar line of thinking has been presented already by Hashizume (1970)[4], though his discussion on the geological significance of this phenomena seems not to be sufficient. He has estimated the angle between the fault plane of microearthquakes and the axis of the real compression, based on the abundant data from the microearthquake observation stations. As far as the geologic interpretation of this phenomena is concerned, the result obtained by Yamashina (1973)[5] is noteworthy. He discussed the orientation of conjugate fractures and magnitude of the dihedral angle, on the basis of the angular fluctuation of the *P*-axes of the Matsushiro earthquake swarm.

It is frequently encountered in the rock specimen fractured experimentally and in field survey of joints, minor faults and large active faults that fracturing occurs along the plane crossing the applied maximum compression with an angle less than 45°. Therefore, it may be reasonable to infer that faulting accompanied with earthqaukes also occurs along the plane which declines with an acute angle to the axis of the maximum compression.

The first purpose of this paper is to settle the statistical foundation of this inference. Then, we wish to evaluate the fracture angle of faults generating earthquakes in the crust of the Kinki district, Southwest Japan, on the basis of the seismological reports on focal mechanisms such as Ichikawa (1965), Hashizume (1970) and Nishida (1973)[6].

Of course, another interpretation than this one may be possible. Nevertheless, it can be emphasized here that among some interpretations, the present one seems reliable and useful, especially when the relation between seismicity and fault activity in such a region as the Kinki district is discussed in connection with development of the geological conjugate fractures.

## 2. Conjugate Fracture

The deformational mode of rocks as shown in Fig. 1 depends on such numerous factors as confining pressure, strain rate, temperature, etc. as compactly summarized by Hoshino (1966)[7]. As far as the brittle fracturing with release of strain energy is considered, the failure occurs on the plane which is oblique to the maximum principal (compressive) stress axis, $\sigma_1$, and includes the intermediate one, $\sigma_2$. The fracture angle, $\theta_0$, measured from $\sigma_1$ to the plane is nearly equal to zero when the extention fracture is considered (Griggs & Handin, 1960)[8]. In the case of shear fracture, $\theta_0$ is much greater than zero.

A fault is a plane of failure which exhibits obvious signs of differential movement of the rock mass on one or either side of the plane. If there is scarcely any evidence

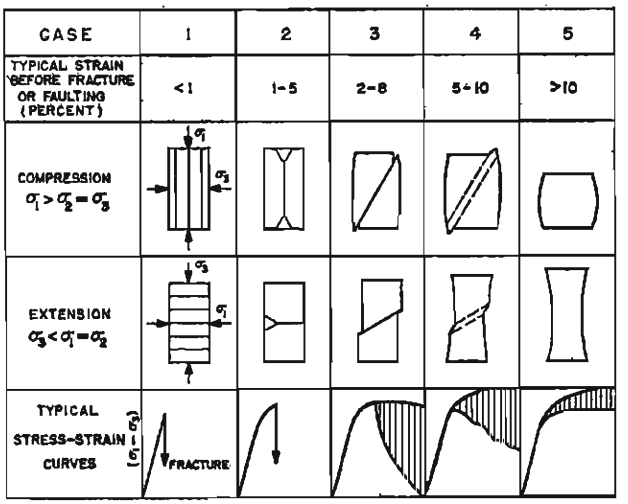


Fig. 1. Schematic representation of the spectrum from brittle fracture to ductile flow, with typical strains before fracture and stress-strain curves for uniaxial compression and extension. Case 1; extension fracture, case 3; fault, case 5; uniform flow, case 2; coexistence of extension fracture and fault and case 4; ductile fault. After Griggs & Handin (1960)[8].

of the movement, the fracture is usually called a joint. Faults are and joints may be, therefore, the plane of shear failure. Two intersecting shears, that is, conjugate or complementary shears, are encountered occasionally at a geologic survey in the field, though one of the shears develops in the experimentally deformed specimen. A joint of shear origin is genetically the same as that of a fault (Hirano, 1970b)[9]. An example of a conjugate joint in the field is given in Fig. 2.

Fault set is classified into thrust, normal fault and strike-slip fault, according to the attitude of the principal stress axes to the horizontal ground surface (Anderson, 1951)[10]. When thrust is considered, $\sigma_1$ and $\sigma_2$ are horizontal and $\sigma_3$ is vertical. Likewise, $\sigma_2$ and $\sigma_3$ are horizontal against the vertical $\sigma_1$ in a normal fault. However, a strike-slip fault has vertical $\sigma_2$ with horizontal $\sigma_1$ and $\sigma_3$. This paper is chiefly concerned with strike-slip faults

Shear fracture in the rock specimens under compression test occurs along a plane which makes an angle not of 45° but less than 45° with the axis of maximum compression. Experimental results on granitic rocks are represented in Fig. 3. In field observations, fault planes of a conjugate set also form an acute angle. The example of shear joint shown in Fig. 2 represents also the same condition (Fig. 4). The acute angle which exists between complementary shears is, in fact, predicted by the Navier-Coulomb criterion of brittle failure as follows.

The Navier-Coulomb criterion of brittle failure is based upon the concept that failure will take place along a surface when the shear stress, $\tau$, acting in that plane is sufficiently large to overcome sum of the cohesive strength, $\tau_0$, of the material and

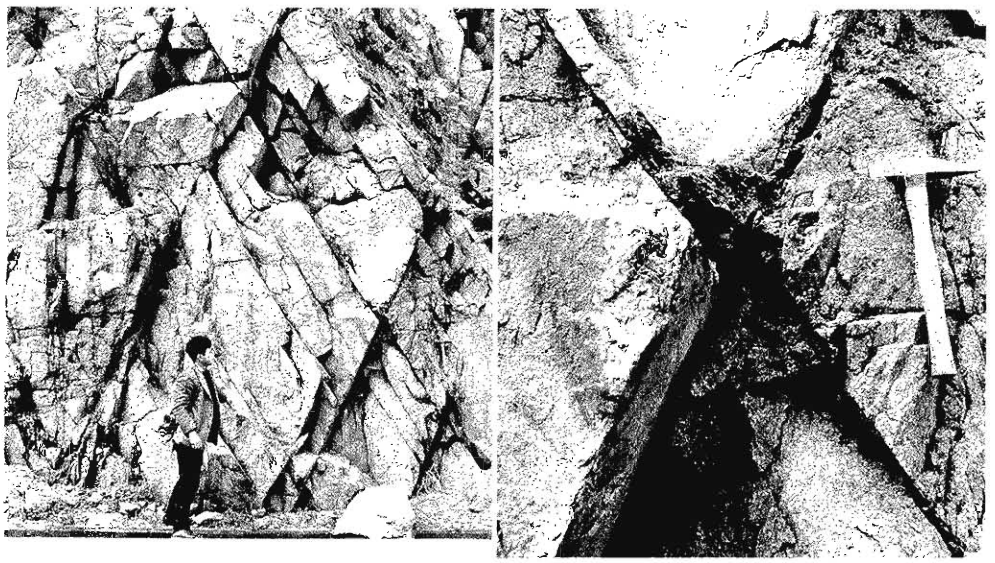

Fig. 2. An example of a conjugate joint in the Rokko Mountains. Photo at the right is a partial enlargement of the left one.

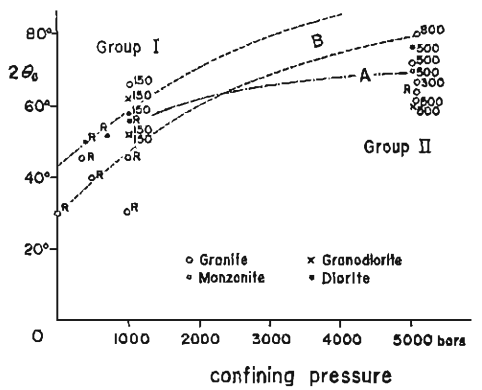


Fig. 3. Relationship between dihedral angle, confining pressure and temperature for granitic rocks. Constructed from Griggs et al. (1960)[11], Handin (1966)[12], Robertson (1955)[13], Mogi (1964)[14] and Borg & Handin (1966)[15]. Numerals on data point give temperature. R shows experimental data in room temperature. Group I and II correspond to the shallow and deep conditions, respectively. After Hirano (1971a).

frictional resistance to movement which is said to equal the stress normal to the shear surface, $\sigma_n$, multiplied by coefficient of internal friction, $\mu$. Thus, the failure criterion may be expressed as,

$$\tau = \tau_0 + \sigma_n \mu. \tag{1}$$

Consider a plane in a stress field, of which maximum and minimum principal com-

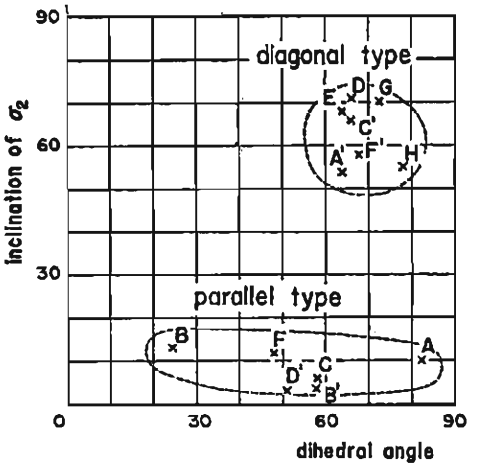


Fig. 4. Dihedral angle of conjugate shear $2\theta_0$ and inclination of the intermediate compressive axis, $\sigma_2$, derived from the conjugate joint systems of the Rokko Mountains (Hirano, 1971b).

pressions are $\sigma_1$ and $\sigma_3$, respectively. When the plane makes an angle $\theta$ with the axis of $\sigma_1$, the normal stress, $\sigma_n$, and shear stress, $\tau$, acting on the plane are given by

$$\sigma_n=\frac{\sigma_1+\sigma_3}{2}-\frac{\sigma_1-\sigma_3}{2}\cos 2\theta \tag{2a}$$

$$\tau=\frac{\sigma_1-\sigma_3}{2}\sin 2\theta, \tag{2b}$$

respectively. The maximum shear stress occurs when $\sin 2\theta=1$ or $2\theta=90°$. When $\sin 2\theta=-1$ or $2\theta=-90°$, $-\tau$ is also maximum.

Further by simple calculation, one obtains that the optimum condition for shear occurs when

$$\tan 2\theta=\pm 1/\mu, \tag{3}$$

if the internal friction is taken into account. The angle between the plane of fracture and $\sigma_1$ is given by

$$\theta_0=45°-\phi,$$

where $\phi$ is the angle of internal friction and $\tan\phi=\mu$. Taking account of symmetry of a stress field, the angle which exists between complementary fault system, $2\theta_0$, is

$$2\theta_0=\pm 90°\mp\phi \tag{4}$$

and $2\theta_0=\pm 90°$ when $\mu=0$. Thus, the Navier-Coulomb criterion is in agreement with both experimental data in laboratory and geologic data in the field. From the measured values of angles of fractures in test specimens and dihedral angles between complementary fault systems, one can find out easily the value of $\mu$.

Very shallow earthquakes are the result of shear failure in the Earth's crust. Therefore, it is reasonable to consider from geologic and experimetal evidence that fractures accompaning earthquakes also make angles not equal to 45°, but less than 45° with the axis of the maximum tectonic compression. In the following sections, we will discuss the angle of fracture and the effect of $\mu$, using the seismic data. Discussion is concerned chiefly with the fractures of strike-slip type which develop in the Kinki district where a dense network of stations for microearthquake observation has been established.

## 3. Focal Mechanism and Fracturing

Seismic waves are elastic ones generated by shear failure of rocks in the crust and, maybe, in the upper mantle. When *P*-waves arrive at an observation station, the Earth's surface moves initially towards or oppositely to the focus of the earthquakes according to the azimuth from the origin to the station. Spatial distribution of the initial motions of *P*-waves is concerned with the geometry of mechanical motion at the origin, i.e. focal mechanism.

The radiation pattern of the initial motions of *P*-waves is divided into the compressional quadrants and dilatational ones by two planes intersecting at right angle, that is nodal planes, and such a radiation pattern is said to be the quadrant type. Methods of determining the nature of the motions at the foci of earthquakes have been developed by many seismologists (Hodgson, 1959[17], 1961[18], Honda, 1962[19]).

Honda (1962) proposed the well known force system of type II (double couples) as a mathematical model of the motion at the focus, which has been accepted widely now. This model is expressed by two kinds of equal force system, i.e. (a) a pair of two forces without moment acting at right angles to one another and (b) a pair of coplaner couples acting at right angles to one another (Fig. 5).

In the case of model (a), the forces toward the focus are termed the principal compression and their direction as the axis of principal compression or the *P*-axis. The opposing forces and their direction are principal tension and the axis of principal tension or the *T*-axis, respectively. If the *P*-axis is nearly parallel to that of the tectonic maximum compression, $\sigma_1$, in an area, we can obtain the tectonic stress field on the basis of the radiation pattern of *P*-waves from earthquakes occurring in the area concerned. In fact, studies on the radiation pattern of *P*-waves have provided a lot of significant information on tectonic stresses acting presently in the crust and upper mantle.

The model (b), equivalent to (a), is important especially when the relation between earthquake and fault is considered. Because, this model suggests implicitly that one of the nodal planes may be regarded as the plane of faulting accompanying the earthquake.

Maruyama (1963) correlated exactly the nodal plane with a plane of faulting based on the elastic theory of dynamic dislocation[20]. He showed that the radiation pattern of *P*-waves due to discontinuities of displacement components corresponding to a slip on a small dislocation surface was the same as that due to the force system of type II (Fig. 6). In fact, it has been confirmed by geologic, geodetic and seismological survey around the epicenter that earthquakes, at least large ones, are due to shear fractures in fresh rocks or, most frequently, slips along the pre-existing faults.

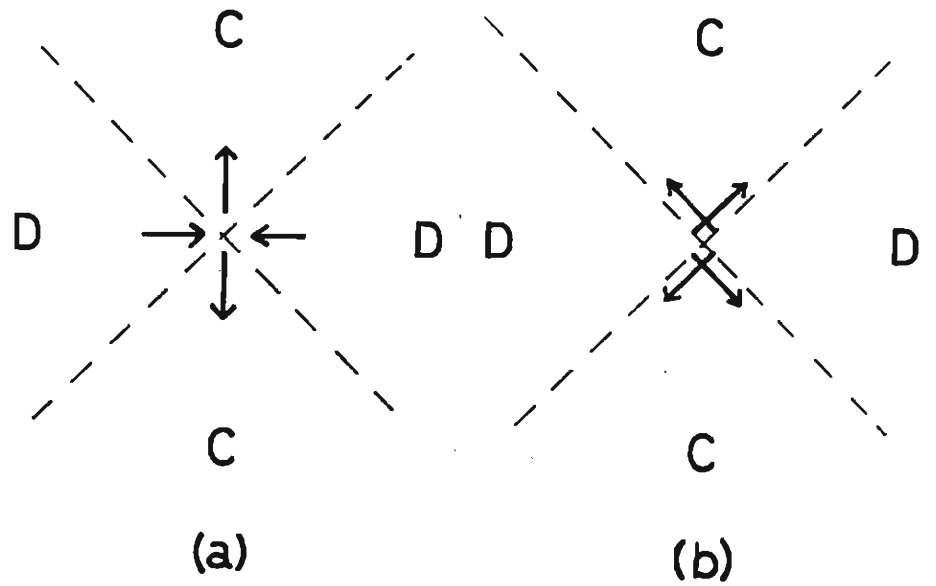


Fig. 5. Double couple model. (a); a pair of two forces without moment and (b); a pair of two forces with equal moment. Both force systems are equivalent to each other. In the quadrants shown by C and D, compressional (push) and dilatational (pull) initial motions are observed, respectively. Broken lines show nodal lines.

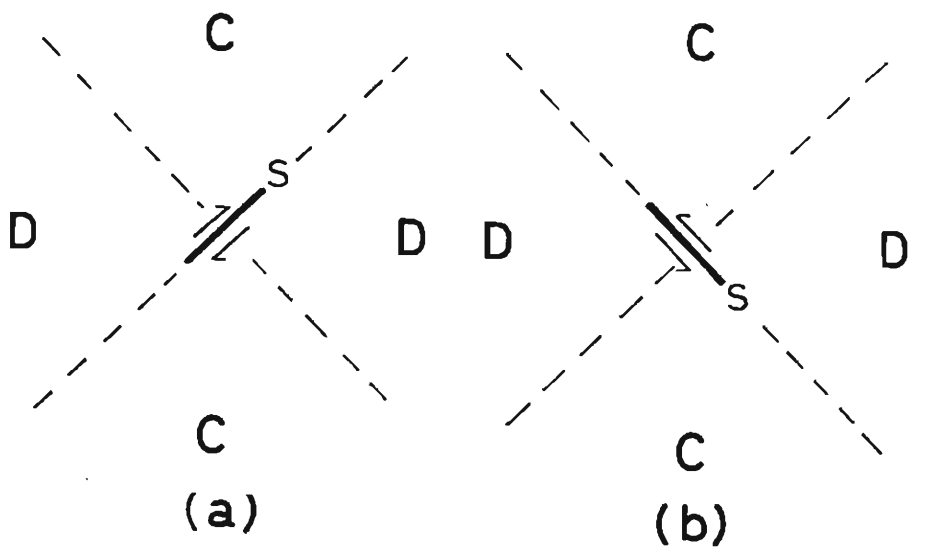


Fig. 6. Dislocation model. (a); a right-lateral slip on a small dislocation surface S and (b); a left-lateral slip. Both types of slip generate the same radiation field of initial motions. Note that one of the nodal planes coincides with the dislocation surface.

Thereby, the plane of faulting has been regarded as being identical with one of the nodal planes in fault plane solution.

So far as dislocation theory by Maruyama (1963) is concerned, it is inevitable that the nodal planes intersect one another at right angle. If the orientation of *P*-axis is constant, earthquake faults in a conjugate set might be always intersecting at right angle. This seems not concordant with the observations on the geologic fault, which were considered in the previous section. This contradiction leads us a singificant aspect on a relation between faulting and focal mechanism as follows.

If shear fractures might always occur along the planes which make an angle of 45° with the axis of tectonic compression in the crust, the *P*-axes might be parallel to the axis of tectonic compression. However, as shown in the case of experimental fractures in rock specimens and geologic faults, it is more reasonable to consider that fracturing occurs generally along the planes intersecting the tectonic compression at angles less than 45°. Then, the *P*-axis is not necessarily parallel to the axis of regional compression but drifts by $45°-\theta_0$, when $\theta_0$ denotes an angle between the fault plane and the tectonic stress axis. These angular relations are summarized in Fig. 7, following Yamashina (1973)[5].

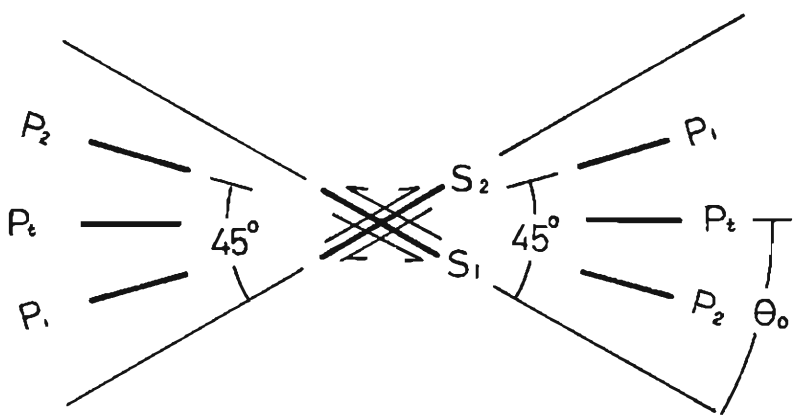


Fig. 7. Schematic diagram showing the relation between tectonic compression, strike-slip faults and the P-axes derived from the radiation patterns. $P_t$ gives the orientation of the tectonic compression. $P_1$ and $P_2$ are the P-axes obtained from the radiation patterns of initial motions due to slips along the fault planes $S_1$ and $S_2$, respectively.

Therefore, it is hoped that statistical study of these departures of the *P*-axes from the tectonic stress axis provides us a key with which we may infer the nature of fracturing in the crust and estimate the angle of conjugate fractures and the effect of internal friction in the actual rocks. From this point of view, let us review the papers concerning the focal mechanisms chiefly of the Kinki district such as Ichikawa (1965)[2], Hashizume (1970)[4] and Nishida (1973)[6] and try to estimate the orientation of the axis of tectonic compression $\Phi$, fracture angle $2\theta_0$ and coefficient of internal friction $\mu$ in the following sections.

## 4. Bimodal Distribution of the *P*-axis

Ichikawa (1965) gave the *P*-axes of small earthquakes which occurred in Southwest Japan during the period from 1926 to 1962 on the basis of the initial motions of *P*-waves observed at the seismological stations of the Japan Meteorological Agency (Fig. 8)[2]. Following this result, the angular distribution of the *P*-axes presents two maximum peaks at both sides of the E–W direction (Fig. 9). The fact leads us to the inference that shear fracturing accompanying small earthquakes may occur along the planes which make an angle less than 45° with the stable axis of regional compression. Bimodal distribution of the *P*-axes is also clear on the Matsushiro earthquake swarm.

Orientation of *P*-axes shows indeed a wide fluctuation and this can correspond to that of the trend of the faults as well as to the dihedral angle. In order to discuss the origin of the bimodal distribution quantitatively and to estimate the angle of fracture,

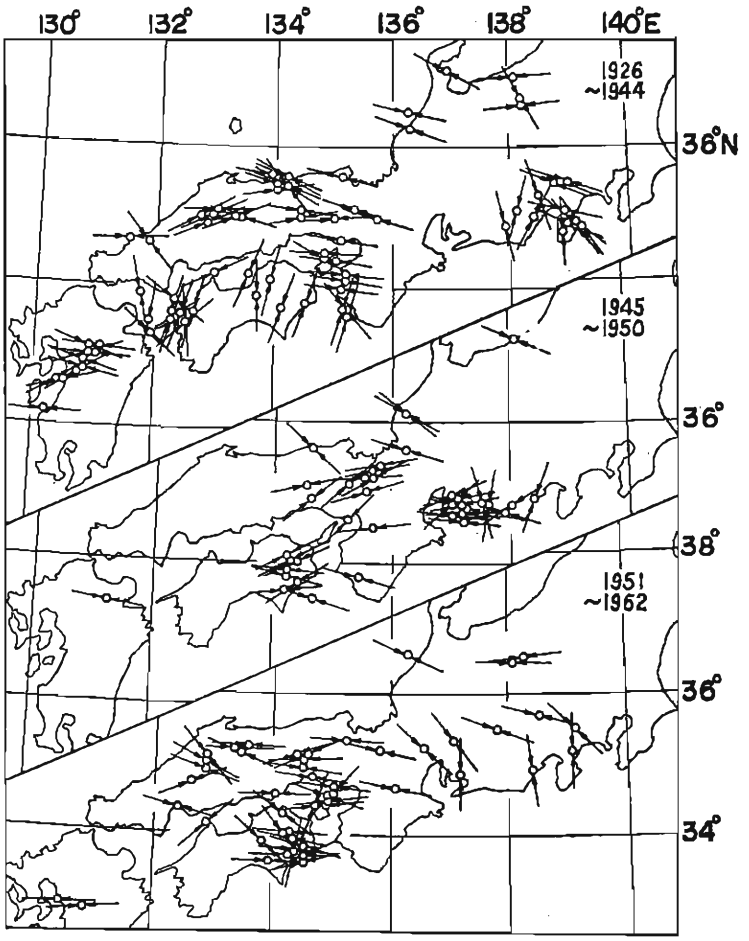


Fig. 8. Distribution of horizontal component of the P-axes in Southwest Japan (Ichikawa, 1965). Obtained from very shallow earthquakes.

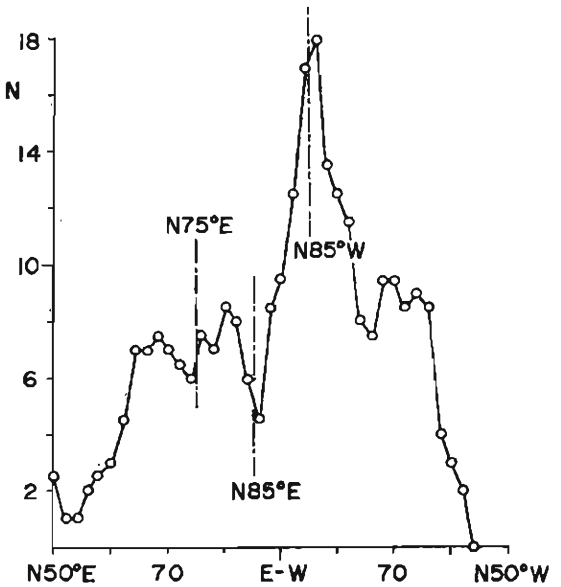


Fig. 9. Summing-up frequency distribution of the azimuths of the P-axes given by Ichikawa (1965) for very shallow earthquakes in the Inner Zone of Southwest Japan. Only the solutions with vertical null vectors are employed. Each point shows frequency number of the P-axes oriented within an angular interval of 5° from each azimuth.

it is convenient to consider such mathematical models as follows. Let the average value of strikes of fractures with left-lateral and right-lateral slips be $\theta_0$ and $-\theta_0$, respectively. Denoting a function of probability density by $f(\theta)$, we find the probability that a left-lateral slip occurs along a plane with a strike of $\theta$ is given by

$$n^+(\theta)=N_0^+ f(\theta-\theta_0).$$

Likewise, that of right-lateral slip is given by

$$n^-(\theta)=N_0^- f(\theta+\theta_0),$$

where $N_0^+$ and $N_0^-$ are parameters which determine the maximum of $n^+(\theta)$ and $n^-(\theta)$, respectively. The ratio $r=N_0^+/N_0^-$ plays an important role in the following discussion.

As we are treating only the case of the strike-slip fault, the $P$-axis is horizontal and oriented in direction rotated by 45° counterclockwise from the plane along which the slip occurs for the case of a left-lateral slip. For the case of right-lateral slips, $P$-axis rotates by 45° clockwise. Then, probability density of direction of the $P$-axis $p(\theta)$ and the $T$-axis $t(\theta)$ can be expressed by

$$p(\theta)=n^+(\theta+45°)+n^-(\theta-45°) \tag{5}$$

$$t(\theta)=n^+(\theta-45°)+n^-(\theta+45°), \tag{6}$$

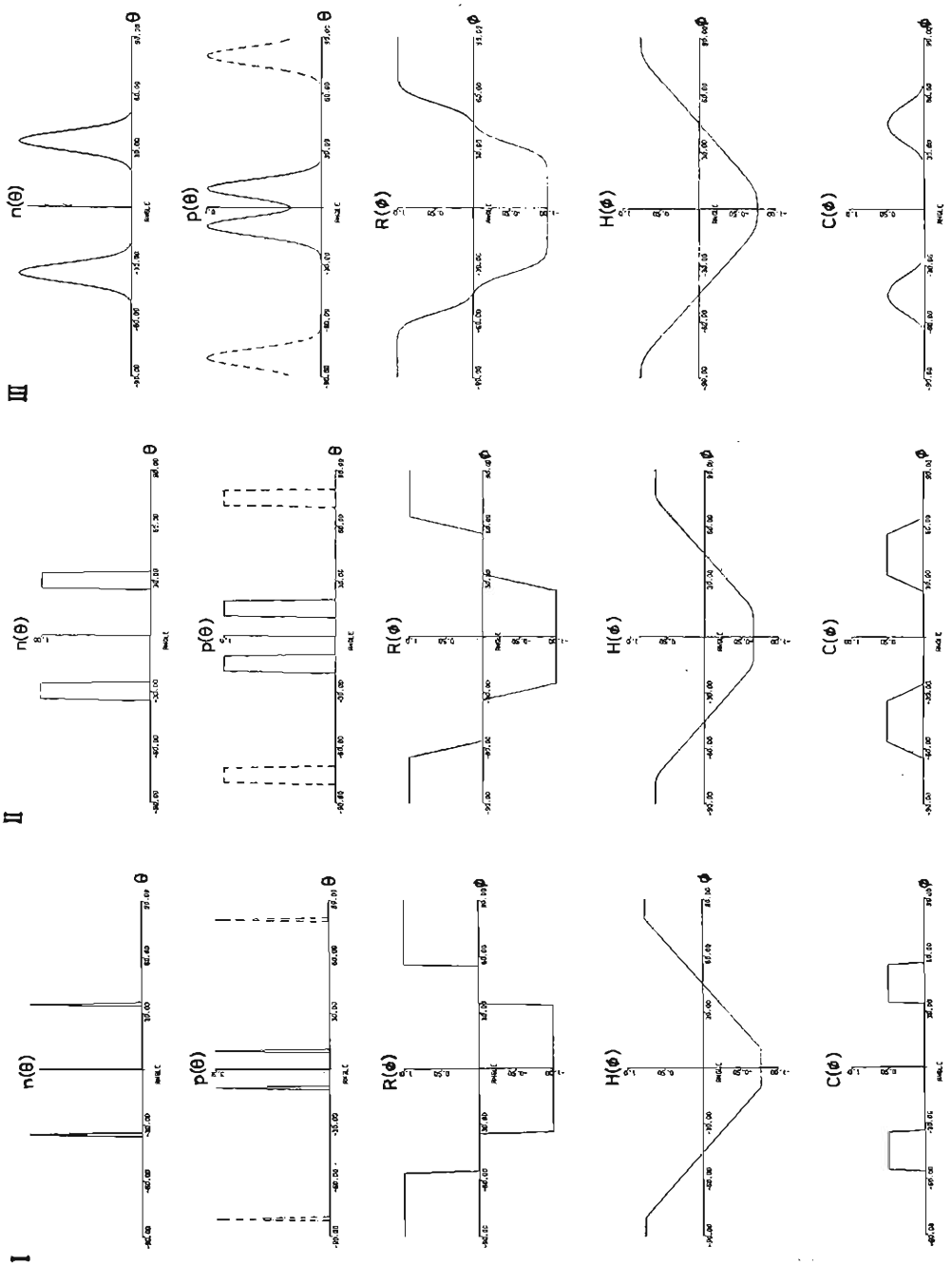


Fig. 10. Theoretical curves of fracture system $n(\theta)=n^{+}(\theta)+n^{-}(\theta)$, probability density of the P- and T-axes $p(\theta)$ (fine curves) and $t(\theta)$ (broken curves), radiation pattern $R(\psi)$, convolution $H(\psi)$ and inconsistent ratio $C(\psi)$. Case I; $2\theta_0=70°$ and $r=1$, case II; $2\theta_0=60°$, $r=1$ and $\sigma=5°$ and case III; $2\theta_0=70°$, $r=1$ and $\sigma=5°$.

respectively. Fig. 10 shows theoretical curves of $p(\theta)$ and $t(\theta)$ for three cases of I, II and III, where functions of probability density are assumed to be a delta function, a rectangular shaped function with a width $2\sigma$, and normal distibution $N(0, \sigma^2)$, respectively.

In each case, it is evident that peaks appear at both sides of $\theta=0°$ when $2\theta_0 \neq 90°$, and that the directions at which $p(\theta)$ becomes maximum differ from that of the axis of maximum compression. Therefore, it is necessary to distinguish the direction of the axis of regional compression from two prominent directions of the *P*-axes. The former must be estimated by a bisector of the latter. However, separation of the two peaks is no good when $2\theta_0$ closes into 90°, even if $2\theta_0<90°$. In Fig. 11, curves of $p(\theta)$ are illustrated in the right for various values of $2\theta_0$. Even if the angular distribution of the *P*-axes is apparently unimodal, it is not always correct to conclude that $2\theta_0=90°$.

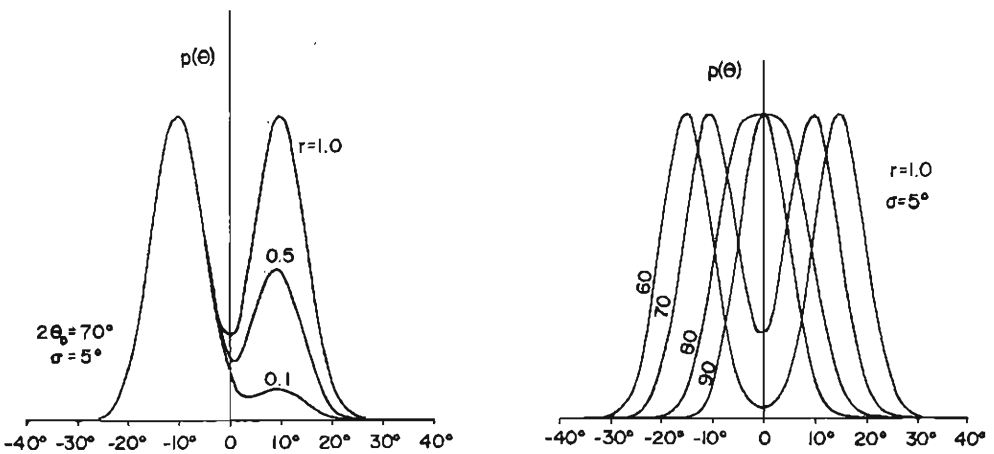


Fig. 11. Left; theoretical curves of $p(\theta)$ for various values of $r$. Case III, $2\theta_0=70°$ and $\sigma=5°$.
Right; theoretical curves of $p(\theta)$ for various values of $2\theta_0$. Case III, $r=1$ and $\sigma=5°$. The result means that most frequent orientation of the *P*-axes differs from that of the axis of tectonic compression. The two peaks become less separable with increasing values of $2\theta_0$.

As the *P*-axes of small earthquakes given by Ichikawa (1965) have two dominant directions, it can be inferred that these earthquakes were associated with slips along the fault planes forming a conjugate pattern which intersect at angles less than 90° with each other. An angular interval between two dominant directions of the *P*-axes may be estimated to be about $2\theta_0$ from Fig. 9. This means that $2\theta_0=70°$ and $\mu=0.36$. The axis of regional compression in the Inner Zone of Southwest Japan is estimated to be almost at the E–W direction (actually N85°E) as shown by the bisector of the dominant directions of the *P*-axes.

Relative height of the peaks in frequency distribution may be related to such dominancy of the respective faults composing a conjugate set as given by paramenter $r$, effect of which is given in the left of Fig. 11. From this point of view, Fig. 9 as well

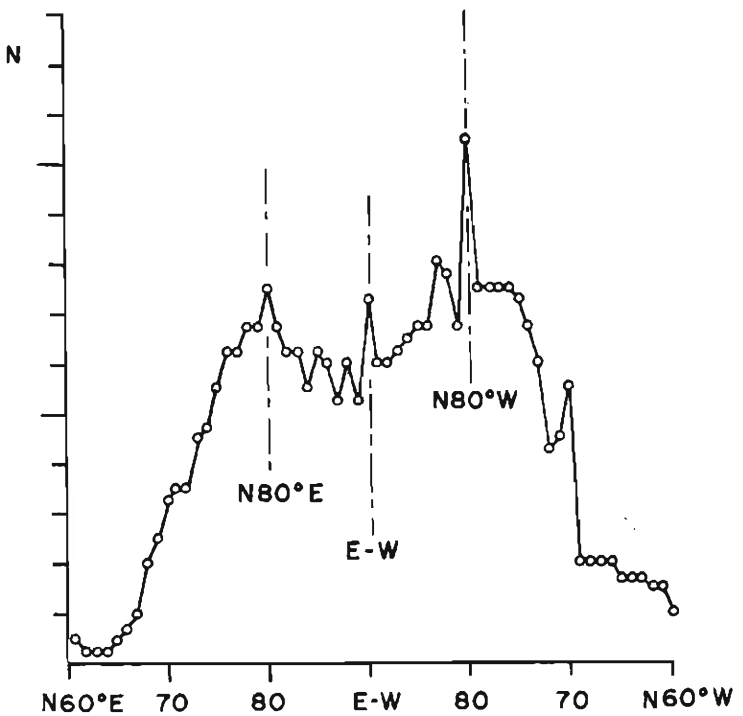


Fig. 12. Frequency distribution of azimuth of the *P*-axes given by Ichikawa (1969) for Matsushiro swarm. Redrawn from Yamashina (1973), who concluded from this figure that $2\theta_0=70°$ and $\mu=0.36$.

as Fig. 16 also represents predominancy of the faults of NE–SW direction in the Kinki district.

When we were preparing this report, Yamashina (1973)[5] also pointed out independently that there existed two peaks in the angular distribution of the *P*-axes given by Ichikawa (1969)[3] for small earthquakes belonging to the Matsushiro earthquake swarm (Fig. 12). According to his estimation, $2\theta_0=70°$ and $\mu=0.36$ as regard to the compressional axis of E–W direction. Yamashina also suggested that the peak around N80°E corresponded to slips along the buried left-lateral fault running in N55°W, which was offered by Nakamura & Tsuneishi (1967)[21] on the basis of field survey and measurement of the surface fissures by instruments. The other peak around N80°W is suggestive of the existence and activity of the fault which forms a conjugate set with the former one. The elliptic area of seismic activity extending in a NE–SW direction may involve this fault, though no surface evidence shows the existence of this one.

## 5. Fluctuation of Fault Strikes and Superposition of the First Motions

Precise estimation of the values of $2\theta_0$ should be based on a number of observational data from numerous earthquakes. Densely distributed seismological stations with

high sensitive instruments have provided enough data to satisfy this condition. A detailed study on the radiation patterns of initial motions from microearthquakes gives us the important information concerning the value of $2\theta_0$.

On the basis of data of *P*-waves initial motions observed at the Tottori Microearthquake Observation Station, Disaster Prevention Research Institute of Kyoto University, Hashizume (1970) discussed focal mechanisms of the microearthquakes which occurred in the northwest part of Kinki district during the period from 1964 to 1968[4]. He determined the axis of regional compression to be N85°E. Assuming the radiation pattern which has a vertical null vector and such an axis of compression as given above, he counted the number of the inconsistent initial motions to the pattern at each 2° interval of the azimuth. The ratios of the number to total number of data are represented in Fig. 13. As given in this illustration, the ratio becomes 0.5 very close to 45°, and Hashizume (1970) concluded that $2\theta_0=90°$. Accordingly, the coefficient of internal friction $\mu$ in the crust might be regarded to be nearly equal to zero.

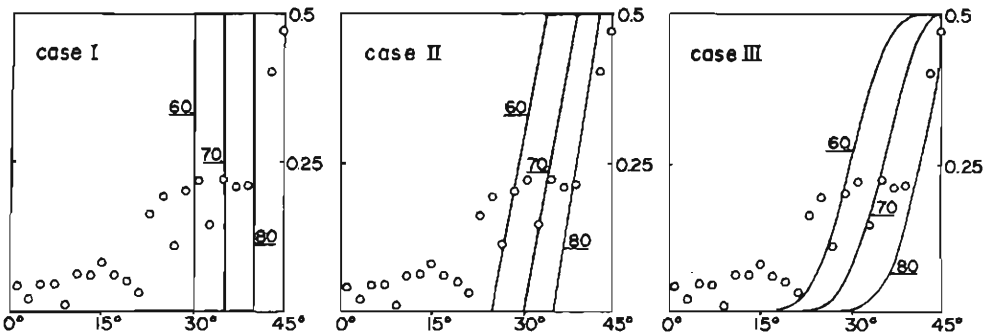


Fig. 13. Observed and theoretical ratios of inconsistent data to the sampling numbers for the assumed radiation pattern. The observed ratios (open circles) are redrawn from Hashizume (1970). In his calculation, the assumed radiation pattern is constructed so that the *P*-axis is oriented in N85°E direction. Theoretical curves of $C(\psi)$ are illustrated by thick lines for case I, II and III, respectively. The data seem to show better fits to the curves of case II and III.

This result is somewhat extreme to be accepted, as geologic evidence shows that conjugate faults intersect each other at angles less than 90°. From this connection, we are interested in examining whether there are other methods to interpret the data that he employed.

In order to discuss the radiation pattern and the related problem quantitatively, the mathematical model proposed in the previous section is convenient. Let us consider a compressional and a dilatational motion which arrive at a station of azimuth $\psi$ as $+1$ and $-1$, respectively, in the same manner as Hashizume (1970). When a left-lateral slip occurs along a plane with a strike $\theta$, the radiation pattern of *P*-waves can be expressed by $g(\psi-\theta-45°)$, where $g(\theta)$ is a function expressed by $g(\theta)=\text{sign}\ (\cos 2\theta)$. In the same manner, the radiation pattern from a right-lateral slip can be expressed by $g(\psi-\theta+45°)$. As left- and right-lateral slips occur with

the probability of $n^+(\theta)$ and $n^-(\theta)$, respectively, the difference between the number of compressional motions and that of dilatational ones, noted by $S(\psi)$, is given by

$$S(\psi)=\int_{-90}^{90}[n^+(\theta)\,g(\psi-\theta-45°)+n^-(\theta)\,g(\psi-\theta+45°)]\,d\theta. \tag{7}$$

Dividing $S(\psi)$ by total number of fractures $N$, expressed by

$$N=\int_{-90}^{90}[n^+(\theta)+n^-(\theta)]\,d\theta,$$

we have

$$R(\psi)=S(\psi)/N \tag{8}$$

which is one of the mathematical expressions of superimposed push-pull distribution. $R(\psi)$ varies from $-1$ to $+1$. $R(\psi)=+1$ and $-1$ mean that only compressional and dilatational waves arrive at the station of the azimuth $\psi$ respectively, and $R(\psi)=0$ means that both waves are observed at an equal chance. For the three cases of I, II and III, curves of $R(\psi)$ are calculated with $2\theta_0=70°$ or $60°$, $\sigma=5°$ and $N_0^+=N_0^-$. The results are represented graphically in Fig. 10.

Denoting the azimuth of a station by $\psi$ as before, $C(\psi)$ is defined by

$$C(\psi)=[R(\psi)\,g(\psi)+1]/2 \tag{9}$$

which gives the probability of observation of inconsistent motions with the radiation pattern whose $P$-axis is oriented in the direction of $\psi=0°$. It is noted here that the nodal lines are trending in the direction of $\psi=\pm45°$. As the function $C(\psi)$ in case of $N_0^+=N_0^-$ is symmetric with respect to the axis of $\psi=0°$ and $\pm45°$, it is sufficient to discuss the characteristics of $C(\psi)$ in the interval from $\psi=0°$ to $45°$.

$C(\psi)$ for various values of $2\theta_0$ is also given in Fig. 13. In case of I, $C(\psi)$ changes suddenly from 0 to 0.5 at the angle of $\psi=\theta_0$. In both cases of II and III, $C(\psi)$ increases gradually to 0.5. As easily understood from the definition of $C(\psi)$, an increasing rate of $C(\psi)$ diminishes in pace with the increase of $\sigma$. As shown by this result, it is only in the case of I that the ratio of inconsistent data approaching abruptly to 0.5 at the angle $\theta_0$ takes place. It is severe to conclude from comparison among points and theoretical curves in Fig. 13 that $2\theta_0$ was 90° or, at least, nearly equal to 90°, unless the case of I is concerned.

By analogy to other natural phenomena, it seems more reasonable to take into account of the probable scatter of the orientation of fractures as shown by the case of II and III. The data by Hashizume (1970) seems to show a better fit to the theoretical curves of $C(\psi)$ obtained in the cases of II and III. From this point of view, it may be reasonable to consider that his conclusion on $2\theta_0$ is not necessarily an abusolute one and his data should be interpreted accordingly.

From Fig. 13, we can estimate the value of $2\theta_0$ so that the observed data fits most suitably to theoretical curves. The estimated values are $2\theta_0=70°$–$80°$ in case of II, and $2\theta_0=70°$–$80°$ in case of III. The estimated valuse of $2\theta_0$ is a fairly good agreement with that derived from geologic survey and experiments of rock fracturing, though there might be some scale effect on the physical properties of the rocks.

Judging from this value, the coefficient of internal friction in the crust is found to be $\mu=0.2$–$0.4$.

## 6. Local Drift of the Orientation of the *P*-axis

In order to estimate the mean orientation of the axis of regional compression in northwest Kinki, Hashizume (1970) calculated the convolution of the $R(\phi)$ of the observed initial motions with the function $g(\phi)$. Nishida (1973)[6], one of the present writers, used the method of smoothing radiation pattern developed by Aki (1966)[22]. Both methods are quantitative expressions of the so-called superimposed push-pull distribution and are equivalent to each other, as far as a two-dimensional radiation pattern is concerned.

As $R(\phi)$ and $g(\phi)$ are periodic functions, convolution of $R(\phi)$ with $g(\phi)$ is expressed by

$$H(\phi)=\frac{1}{180}\int_{-90}^{90} R(\theta)\, g(\phi-\theta)\, d\theta, \tag{10}$$

where the convolution is divided by 180° in order to be normalized. Based on the number of compressions, $N^+$, and dilatations, $N^-$, within the angular interval of 45° from a point of the azimuth $\phi$, the smoothed radiation pattern can be calculated in the form of the normalized parameter $K(\phi)$, which is defined by

$$K(\phi)=\frac{N^+-N^-}{N^++N^-}. \tag{11}$$

In both methods, the minimum point defines the mean orientation of the *P*-axis.

When we have data concerning initial motions but can not determine the fault plane solution of each earthquake, the average orientaion of compression is inferred by these methods. The result is justified when both fractures composing a conjugate set are equally developed and $N_0^+=N_0^-$. From this point of view, the tectonic compressive axis of N85°E found by Hashizume (1970) for the Kinki district should be accepted. On the other hand, it happens that *P*-axis deflects locally from the direction of the tectonic compression, if one of the conjugate faults develops dominantly. Therefore, it is necessary to take into account of the apparent drift of the average *P*-axis when $N_0^+\neq N_0^-$. Such a situation is typically presented in the case of the *P*-axis derived from fault plane soltuion of individual earthquakes. Apparent drift of the *P*-axis due to a different value of $r=N_0^+/N_0^-$ is shown graphically in Fig. 14.

Based on this conclusion, let us interpret the local deflection of the *P*-axis given by Nishida (1973). Fig. 15 illustrates the local orientation of the average *P*-axes at 191 points in the northwest Kinki district. Each axis shows the orientation of the axis determined on the basis of the initial motions from microearthquakes, which occurred within each $10\times10$ km$^2$ area centering the position of the axis. In Fig. 15, thick and thin axes give the orientations of the reliable and less reliable *P*-axes, respectively. The mean orientation of the *P*-axes are rotated counterclockwise from the E–W direction in the narrow zone containing the major active faults such as the Yamasaki and Mitoke faults, and rotated clockwise in the narrow zone connecting the west part of the River Yodo with the east part of the Awaji Island through the

northern part of Osaka Bay.

The Yamasaki and Mitoke faults have goemorphic evidence showing a left-lateral slip in a recent Age (Huzita, 1969)[1]. Because their general trend is ca. N60°–70°W, it is easily derived that the fracturing accompanying microearthquake occurs dominantly in a left-lateral sense along the plane parallel to the active fault. In such a case, the radiation pattern of seismic waves shows the *P*-axis rotated counterclockwise from an E–W direction (Fig. 15). On the other hand, clockwise rotation of the mean orientation of the *P*-axis in the area southeast of the Rokko Mountains suggests the right-lateral slips along the faults running from the northeast to the southwest, which form a conjugate set with the Yamasaki fault.

Local and systematic rotation of the *P*-axis near the active faults suggests the dominancy of fracturing or slip concordant with the active fault. In the area neighbouring the active fault, dislocations accompanying microearthquakes tend to take place with higher probability along the planes parallel to the fault itself than along the planes obliquely intersecting the fault. Thereby, the dislocation occurs in the same sense as does the active fault.

Fig. 16 shows the summing-up angular distribution of the reliable average *P*-axes shown in Fig. 15. It is clear that there exist two dominant directions near $\psi$=N75°E~N80°E and $\psi$=N85°W. From this illustration, we can estimate the direction of the axis of regional compression, dihedral angle and coefficient of internal friction. The numerical values are

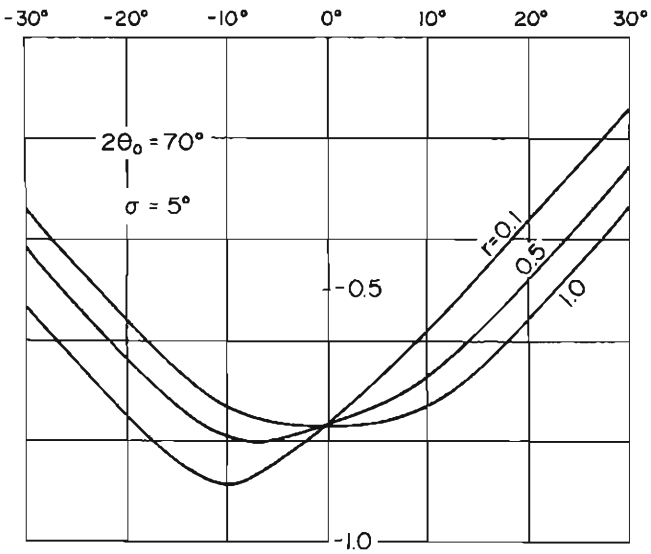


Fig. 14. Theoretical curves of $H(\psi)$ for various values of $r$. Case III, $2\theta_0=70°$ and $\sigma=5°$. Note that the minimum point drifts for an angle of $\theta_0-45°$ with decreasing values of $r$. This means that, when fracturing occurs selectively along planes parallel to one component of the conjugate set, the orientation of the average *P*-axis derived from Hashizume's convolution or Aki's smoothed radiation pattern differs from that of the axis of tectonic compression in the same manner as the *P*-axis of an individual earthquake.

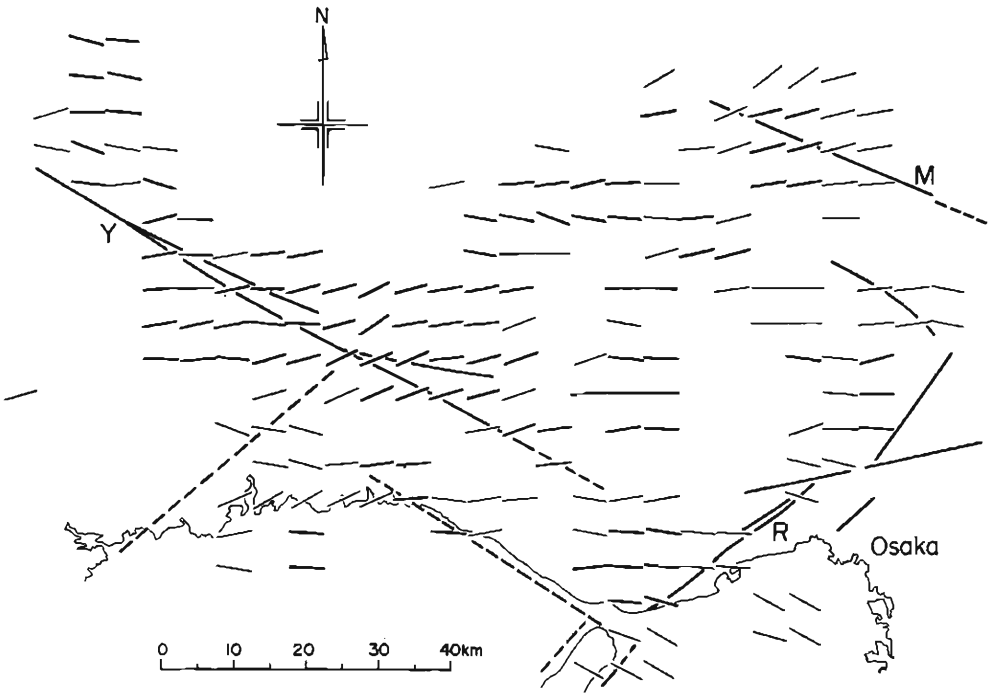


Fig. 15. Distribution of horizontal component of the average *P*-axis in the northwest Kinki district. After Nishida (1973). Each axis shows the mean direction of the *P*-axis determined on the basis of initial motions from microearthquakes which occurred within each 10 km × 10 km area centering the position of the axis. Thick and fine axes show reliable and less reliable solutions, respetively. Systematical fluctuation of the axes is apparent along active faults shown by thick or broken lines. Y; the Yamasaki Fault, M; the Mitoke Fault and R; the Rokko Fault System.

$$\Phi = \mathrm{N85^\circ E}$$

$$2\theta_0 = 70^\circ \sim 75^\circ$$

$$\mu = 0.3 \sim 0.4,$$

respectively. It is interesting that these values are in good agreement with those derived in the previous sections, in spite of the fact that the dihedral angle obtained here only shows the upper limit of the probable value.

Orientation of regional compression is quite similar to that obtained from the records of strainmeters at the tunnel in the Rokko Mountains (Tanaka et al., 1972)[23]. As long as $2\theta_0$ is concerned, the values obtained from the joint survey of the Rokko Mountains (Hirano, 1971b; See Fig. 4)[9] shows good agreement.

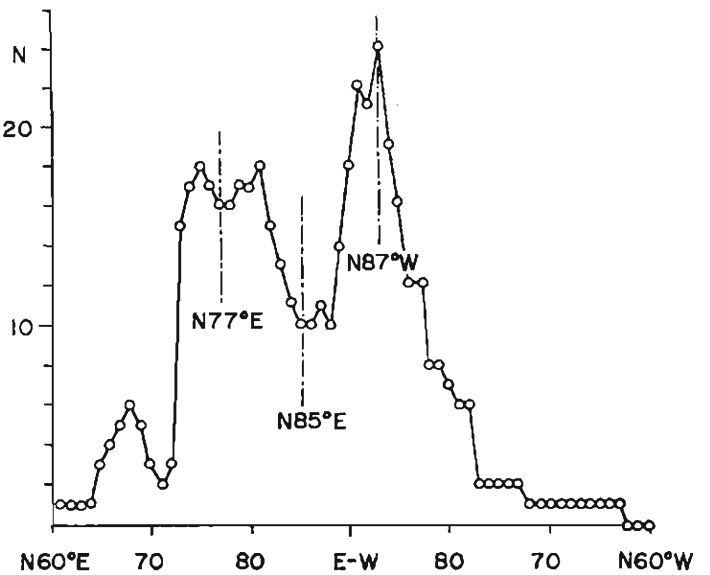


Fig. 16. Summing-up frequency distribution of the azimuths of the reliable average *P*-axes (thick axes in Fig. 15) in the northwest Kinki district. The axis inclining over 15° from the horizontal is excluded. An open circle shows frequency number of the axes oriented within an angular interval of 2.5° from each azimuth.

## 7. Developmental Process of Conjugate Faults

There is often the fact that one of the conjugate fractures develops in the deformed rocks from a laboratory experiment, whereas the faults traced on a geologic map rather occur in a conjugate set. The process through which individual fractures develop into a conjugate set is one of the interesting problems concerning the tectonic history of any area. From this point of view, data of the Matsushiro earthquake swarm serves to provide important information. The activity of the swarm is generally summarized as follows[21,24].

In the first stage (August 1965 to February 1966), epicenters of earthquakes were clustered in a circle 5 km in radius with its center at the northeast of Mt. Minakami. In April and May 1966 (the second stage) the activity was most violent and the seismic area extended to a wider circle. In parallel with violent seismic activity, crustal deformations proceeded in this area. Four ground fissure zones began to be formed linearly in the middle of the epicentral area. The constituent cracks in the zones were arranged uniformly en echelon, indicating the left-lateral movement.

Following a period of low seismicity in June and July, there came another peak of activity (the third stage). The seismic area extended in the NE–SW direction and became elliptical in form with the major axis 28 km long lying in the same direction. Earthquakes decreased in number on the northwest of Mt. Minakami where many cracks developed. Fissure zones began to move again in the same sense as in the previous stage. Moreover, catastrophic landslides occurred due to the unusual outflow of ground waters. Seismic activity decreased rapidly from the beginning of

September 1966 (the fourth and fifth stages). The seismic area took an elliptical form with the major axis 34 km long lying in a NE–SW direction and the minor axis 18 km long in a NW–SE direction.

Based on focal mechanism of these earthquakes, Ichikawa (1969) pointed out that the *P*-axes were in a direction which rotated clockwise from E–W direction in the first stage and that since May 1966 the *P*-axes were generally oriented in N80°–85°E (Fig. 17)[3]. The general trend of the *P*-axes (N80°E) were said to be consistent with the buried left-lateral strike-slip fault offered by Nakamura and Tsuneishi (1968)[21] on the basis of a field survey of ground fissures.

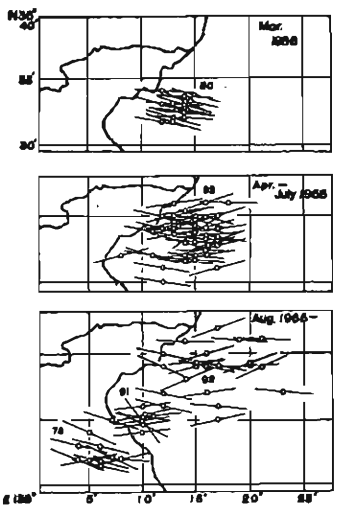

Fig. 17. Distribution of horizontal components of the *P*-axes at each period of Matsushiro earthquake swarm. After Ichikawa (1969). Three periods correspond nearly to the first, second and later stages of activity proposed by Hagiwara & Iwata (1968)[24], respectively.

According to discussion in the previous section and in Yamashina (1973)[5], systematic rotation of the *P*-axes shown in Fig. 17 suggests that fracturing in the first stage occurred prominently along the planes oriented in N55°E direction, and in the second stage, prominently along the planes with a strike of N55°W as seen in the surface fissures. In the following stage, fracturing occurred alternately along the both planes of a conjugate set in the neighbouring areas. These interesting features also suggest that even if conjugate fractures can be regarded to occur with equal probability as a whole, they tend to occur selectively along one component of the conjugate set in a limited period and area.

This fact as well as that given in the previous section leads us to an interesting aspect on the developmental process of the conjugate fractures (Fig. 18). As seen in the case of the Matsushiro earthquake swarm, fracturing occurs in the fresh rock selectively along the plane with a dominant strike and one of the components of a conjugate set is formed beforehand (Fig. 18–A). In the next stage, fractures belonging to

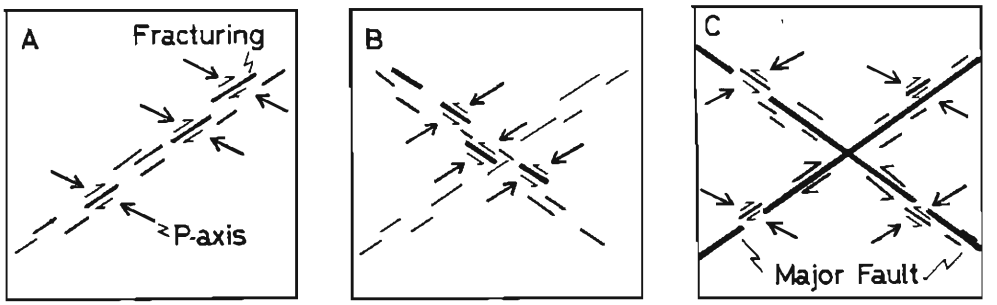


Fig. 18. Schematic diagram showing the developmental process of conjugate faults. A pair of fine arrows shows a sense of slip. Thick opposing arrows show the orientation of the *P*-axis of the earthquake due to the slip. A; selective fracturing along one component of possible conjugate shears, B; complementary fracturing along another component and C; selective fracturing along planes parallel to the neighbouring major active faults shown by thick lines.

another component are formed complementarily (Fig. 18–B). Alternations of the two stages complete the minor and initial conjugate system.

In the following stage, a large fault can be formed along a zone where small fractures are developed densely and there appears the conjugate system of such large scale as to cover all of the Kinki district. Once a large fault is formed, major displacement may take place along the fault and it comes to possess the geomorphic features of an active fault. Fracturing in the neighbouring area of the fault tends to occur prominently along the planes parallel to the fault as seen in the narrow zone along the Yamasaki and Mitoke Faults (Fig. 18–C). Thereby, apparent direction of the maximum compression obtained as the *P*-axis always deflects clockwise or counterclockwise, depending upon the prominent fracturing almost in NE–SW and NW–SE directions, respectively, if the axis of tectonic compression lies in E–W direction.

## 8. Summary Statement

If a fracture accompanying an earthquake occurs along a plane which intersects the axis of tectonic compression, $\sigma_1$, with an angle, $\theta_0$, less than 45°, the *P*-axis derived from the radiation pattern of earthquake drifts by $45°-\theta_0$ from the actual compressive axis. When fractures occur alternately along both planes of possible conjugate shear, there must appear two dominant orientation among the azimuths of the *P*-axes of these earthquakes. The angular interval of two dominant orientations is $90°-2\theta_0$. The axis of tectonic compression must be estimated as the bisector of the two dominant orientations. According to Navier-Coulomb criterion of shear fracture, the value of $2\theta_0$ concerns the coefficient of internal friction, $\mu$, in rocks.

So far as the northern part of Kinki district is concerned, there exist two peaks in frequency distributions of the azimuths of the *P*-axes for small earthquakes given by Ichikawa (1965)[2] and the average *P*-axes for microearthquakes given by Nishida (1973)[6]. As pointed out by Yamashina (1973)[5], the Matsushiro earthquake swarm shows the same tendency. According to these results, the estimated values of $2\theta_0$ and $\Phi$ (orientation of $\sigma_1$) are as follows;

$2\theta_0=70°$ and $\Phi=$N85°E for small earthquakes

$2\theta_0=70°\sim75°$ and $\Phi=$N85°E for microearthquakes

$2\theta_0=70°$ and $\Phi=$N90°E for Matsushiro swarm.

These values of $2\theta_0$ are in good agreement with those obtained from a joint study of the Rokko Mountains[9]. The coefficient of internal friction evaluated from the values of $2\theta_0$ is $\mu=0.3$–$0.4$ for the upper crust.

Hashizume's (1970) convolution method[4] and Aki's (1966) smoothed radiation pattern method[22] give the orientation of the real compressive axis when fractures occur with equal frequency along both planes of possible conjugate shears. There also appears an apparent drift of the estimated axis from the actual compressive axis, unless the equal frequency is maintained. The ratio of inconsistent data given by Hashizume (1970) with the assumed axis of the tectonic compression, N85°E, also suggests $2\theta_0=70°$–$80°$ in spite of his negative conclusion, although the assumed orientation is quite reasonable.

Nishida (1973) showed local orientation of the *P*-axes. Defraction of the *P*-axes near the major active fault suggests that fracturing occurs along the plane parallel to the active fault itself and that sense of dislocation is concordant with that of the fault. This is one of the more advanced views on the relationship between fault and seismic activity than that given by Huzita (1969)[1], who has maintained the linear arrangement of epicenters of microearthquakes along the active fault.

Periodic change of the *P*-axes of Matsushiro earthquake swarm (Ichikawa, 1969)[3] leads us to a significant aspect on the developmental process of conjugate fault system. One of the conjugate fractures develops in the first stage and another is added to the previous one in a later stage. Alternation of two stages may complete a conjugate set.

## Acknowledgements

The writers wish to express their thanks to Professor K. Huzita of Osaka City University and to Professor Y. Kishimoto of Disaster Prevention Research Institute, Kyoto University for generous assistances in the course of the work. Thanks are also due to Dr. M. Hashizume of Okayama University and to Mr. K. Nakagawa of Osaka City University for discussion and suggestion on the problem.

## References

1) Huzita, K.: Tectonic Development of Southwest Japan in the Quaternary Period, Jour. Geosci. Osaka City Univ., Vol. 12, 1969, pp. 53–70.
2) Ichikawa, M.: The Mechanism of Earthquakes Occurring in Central and Southwest Japan, and Some Problems, Papers Meteor. Geophys., Vol. 16, 1965, pp. 104–156.
3) Ichikawa, M.: Matsushiro Earthquake Swarm, Geophys. Mag., Vol. 34, 1969, pp. 307–331.
4) Hashizume, M.: Investigation of Microearthquakes — On Earthquake Occurrence in the Crust —, Bull. Disas. Prev. Res. Inst. Kyoto Univ., Vol. 20, 1970, pp. 65–94.
5) Yamashina, K.: Existence of Internal Friction on the Fault Planes of Earthquakes and its Detecting Method — Mechanics of Faulting — (1), Abstract of the Annual Meeting of Seismological Society of Japan (NO. 2), 1973, pp. 118.

6) Nishida, R.: Stress Field within the Upper Crust Obtained from Focal Mechanism of the Microearthquakes with Reference to the Northwestern Kinki District, Japan, Abstract of the Annual Meeting of Seismological Society of Japan (NO. 2), 1973, pp. 28.
7) Hoshino, K.: Rock Deformation and Geologic Structure, Jour. Geol. Soc. Japan, Vol. 72, 1966, pp. 105–116.
8) Griggs, D. and J. Handin: Observation on Fracture and a Hypothesis of Earthquake, Geol. Soc. Amer., Memoir 79 (Rock Deformation), 1960, pp. 347–364.
9) Hirano, M.: Problems Related to Brittle Fracture in Plutonic Rock with Special Reference to Joints in Granitic Rocks at the Rokko Mountains, Jour. Geol. Soc. Japan, Vol. 77, 1971b, pp. 257–263.
10) Anderson, E. M.: The Dynamics of Faulting and Dyke Formation with Application to Britain (2nd ed.), Oliver & Boyd, 1951, 206p.
11) Griggs, D. et al.: Deformation of Rocks at 50° to 800°, Geol. Soc. Amer,. Memoir 79 (Rock Deformation), 1960, pp. 30–104.
12) Handin, J.: Strength and Ductility, Geol. Soc. Amer., Memoir 97 (Handbook of Physical Constants; Revised ed.), 1966, pp. 223–289.
13) Robertson, E. C.: Experimental Study of the Strength of Rocks, Bull. Geol. Soc. Amer., Vol. 66, 1955, pp. 1275–1314.
14) Mogi, K.: Deformation and Fracture of Rocks under Confining Pressure (1). Compression Test on Dry Rock Sample, Bull. Earthq. Res. Inst., Vol. 42, 1964, pp. 491–514.
15) Borg, I. and J. Handin: Experimental Deformation of Crystalline Rocks, Tectonophysics, Vol. 3, 1966, pp. 249–368.
16) Hirano, M.: Fracture System Expected in a Granite Layer under Lateral Compression, Jour. Geol. Soc. Japan, Vol. 77, 1971a, pp. 171–181.
17) Hodgson, J. H. editor: The Mechanics of Faulting with Special Reference to the Fault Work (A Symposium), Dom. Obs. Pub. Ottawa, Vol. 20, 1959, pp. 251.
18) Hodgson, J. H. editor: A Symposium on Earthquake Mechanism, Dom. Obs. Pub. Ottawa, Vol. 24, 1961, pp. 299–397.
19) Honda, H.: Earthquake Mechanism and Seismic Waves, Jour. Phys. Earth, Vol. 10, No. 2, 1962, pp. 1–97.
20) Maruyama, T.: On the Force Equivalents of Dynamical Dislocations with Reference to the Earthquake Mechanism, Bull. Earthq. Res. Inst., Vol. 41, 1963, pp. 467–486.
21) Nakamura, K. and Y. Tsuneishi: Ground Cracks at Matsushiro Probablly of Underlying Strike-Slip Fault Origin, II. — The Matsushiro Earthquake Fault, Bull. Earthq. Res. Inst. Vol. 45, 1967, pp. 417–471.
22) Aki, K.: Earthquake Generation in Japan for the Years 1961 to 1963 Obtained by Smoothed the First Motion Radiation Pattern, Bull. Earthq. Res. Inst., Vol. 44, 1966, pp. 447–471.
23) Tanaka, Y., M. Hayashi, M. Kato and K. Huzita: Continuous Observation of Crustal Deformations in a Fracture Zone of Rokko Fault System, Bull. Disas. Prev. Res. Inst. Kyoto Univ., Vol. 15B, 1972, pp. 29–41.
24) Hagiwara, T. and T. Iwata: Summary of the Seismographic observation of Matsushiro Swarm Earthquakes, Bull. Earthq. Res. Inst., Vol. 46, 1968, pp. 485–515.